Available online at www.sciencedirect.com
ScienceDirect
Mendeleev Commun., 2020, **30**, 719–721

Mendeleev Communications

Photoinduced solid-state isomerization and structural characterization of a nitro–nitrosyl ruthenium complex with 3-cyanopyridine

Artem A. Mikhailov,* Denis P. Pishchur, Natalia V. Kuratieva and Gennadiy A. Kostin

A. V. Nikolaev Institute of Inorganic Chemistry, Siberian Branch of the Russian Academy of Sciences, 630090 Novosibirsk, Russian Federation. E-mail: amikhailov@niic.nsc.ru

DOI: 10.1016/j.mencom.2020.11.010

The title complex, which is crystallized in a non-centrosymmetric space group due to specific intermolecular interactions, exhibits reversible light-induced nitrosyl linkage isomerism; thus, it is of interest for studying combined Ru–NO ↔ Ru–ON isomerization with non-linear optical properties.

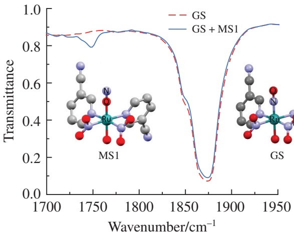

Keywords: ruthenium, nitrosyl, nitric oxide, linkage isomers, photoisomerization, molecular switch.

Ruthenium complexes containing nitrosyl and nitrite ligands possess remarkable photochemical properties manifested in ligand isomerism. A stable Ru–NO (GS) fragment can be changed to Ru–ON (MS1) or/and Ru-η^2-(NO) (MS2) linkages by irradiation with light,[1,2] whereas nitrite complexes can produce nitro (nitrito) isomers.[3,4] Concerning the nitrosyl ligand photoisomerization, in the simplest way, the mechanism of GS transformation to MS1 can be expressed as the two-step process GS → MS2 → MS1, where MS2 is an intermediate state.[5] This isomerization can be applied to assemble materials exhibiting light-triggered magnetic properties[6] and materials suitable for data storage.[7] Recent investigations of the non-linear optical (NLO) properties of nitrosyl ruthenium complexes shows, that NLO response (second harmonic generation) can be driven by the change of NO linkage, thereby providing unique switchable optical properties.[8,9] However, in order to exhibit second harmonic generation, the material should crystallize in a non-centrosymmetric group,[10] which requires specific intermolecular interactions in the structure. Such interactions can be designed by the proper choice of the ligand environment with decent intramolecular charge-transfer. From this point of view, pyridine ligands containing cyanide group are interesting due to separated donor (pyridine ring) and acceptor (cyanide) parts by a conjugated π-system, which can enhance NLO response.[11]

The aim of this work was to study the light-induced nitrosyl linkage isomers of the [RuNO(3-CN-Py)$_2$(NO$_2$)$_2$OH] complex by IR spectroscopy and differential scanning calorimetry (DSC) methods. The structure of the complex was determined by the X-ray diffraction and the intermolecular contacts were investigated by the Hirshfeld surface analysis.

The reaction of [RuNO(NO$_2$)$_4$OH]$^{2-}$ with 2 equiv. of sulfamic acid yielded the [RuNO(H$_2$O)$_3$(NO$_2$)$_2$]$^+$ complex containing labile aqua ligands.[12] The treatment of the reaction mixture with 3-CN-Py gave a precipitate of [RuNO(3-CN-Py)$_2$(NO$_2$)$_2$OH], which was recrystallized from acetonitrile.[†]

Crystal data, structure refinement and chosen bond distances are given in Tables S1 and S2, see Online Supplementary Materials. The crystal structure[‡] is represented by ruthenium octahedrons, in which nitrosyl is in the *trans*-position to hydroxyl ligand. Planar nitrite ligands and 3-CN-Py ligands are in the *cis*-position to each other [Figure 1(*a*)]. The Ru–NO bond length and Ru–N–O angle are typical of Ru^{II}–NO$^+$ complexes [1.769(3) Å and 171.6(3)°, respectively];

[†] *Synthesis of [RuNO(3-CN-Py)$_2$(NO$_2$)$_2$OH].* Na$_2$[RuNO(NO$_2$)$_4$OH]·2H$_2$O (1 mmol) and NH$_2$SO$_3$H (2 mmol) were dissolved in 1 ml of water; after stirring for 30 min, the release of N$_2$ gas was complete, and 3-cyanopyridine (4 mmol) was added. The reaction mixture was stirred for 3 h at 293 K. The resulting yellow powder was filtered off and refined by precipitation from acetonitrile with diethyl ether and then washed with diethyl ether. The yield was 25%. Single crystals suitable for X-ray diffraction were obtained by the slow diffusion of diethyl ether into a solution of the complex in acetonitrile. Found (%): C, 31.9; H, 2.3; N, 21.5. Calc. for C$_{12}$H$_9$N$_7$O$_6$Ru (%): C, 32.2; H, 2.0; N, 21.9. IR at 293 K (ν/cm^{-1}): 3501 (O–H), 2239 (C–N), 1869 (N–O), 1609 (C–C), 1423, 1318 (NO$_2$), 819 (NO$_2$). The powder XRD pattern of the bulk sample corresponds to that calculated from the crystal structure determined by single-crystal XRD.

[‡] *Crystal data for [RuNO(3-CN-Py)$_2$(NO$_2$)$_2$OH].* C$_{12}$H$_9$N$_7$O$_6$Ru, $M = 448.33$, orthorhombic, space group $P2_12_12_1$, $a = 9.9129(3)$, $b = 12.1195(4)$ and $c = 13.7976(4)$ Å, $V = 1657.64(9)$ Å^3, $Z = 4$, $\rho_{\text{calc}} = 1.796$ g cm^{-3}, μ(MoKα) = 0.993 mm^{-1}, $F(000) = 888.0$. 10853 reflections were measured, 3734 independent reflections ($R_{\text{int}} = 0.0291$) were used in a further refinement. The refinement converged to $wR_2 = 0.0540$ and GOF = 1.034 for all the independent reflections [$R_1 = 0.0255$ for 3486 observed reflections with $I > 2\sigma(I)$]. The single-crystal XRD data were collected on a Bruker APEX DUO diffractometer equipped with a 4 K CCD area detector using graphite monochromated MoKα radiation ($\lambda = 0.71073$ Å) at 150 K. The absorption measurements were corrected by the SADABS software. Using Olex2,[27] the structure was solved with the ShelXT[28] structure solution program using Intrinsic Phasing and refined with the ShelXL[29] refinement package using least squares minimization. All non-hydrogen atoms were refined as anisotropic. The hydrogen atom of the OH group was found using an electronic density map. All other hydrogen atoms were calculated in their idealized positions and refined as riding atoms (Table S1).

CCDC 1982496 contains the supplementary crystallographic data for this paper. These data can be obtained free of charge from The Cambridge Crystallographic Data Centre *via* http://www.ccdc.cam.ac.uk.

© 2020 Mendeleev Communications. Published by ELSEVIER B.V. on behalf of the N. D. Zelinsky Institute of Organic Chemistry of the Russian Academy of Sciences.

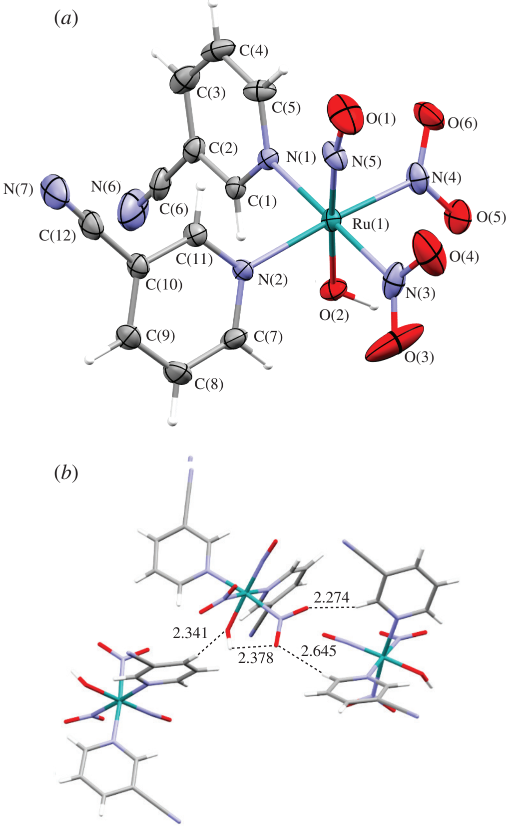

Figure 1 (*a*) Molecular structure of complex [RuNO(3-CN-Py)$_2$(NO$_2$)$_2$OH] (thermal ellipsoids at a 50% probability level). (*b*) Chosen intra- and intermolecular contacts (in Å).

the Ru–NO$_2$ bond lengths are shorter than those of the Ru–N(3-CN-Py) bonds [2.056(4) and 2.068(4) Å *vs.* 2.122(3) and 2.144(3) Å, respectively], which are characteristic of these compounds.[13–16] The angles between the N donor atom of a planar ligand (NO^{2-}, 3-CN-Py), ruthenium and the N(5) atom of nitrosyl ligand are close to 90° (see Table S2). Torsion angles of the 3-cyanopyridine and nitrite ligands are in a range of 17–30° probably due to weak interactions between the oxygen atoms of nitrites and the hydrogens of 3-CN-Py. Figure 1(*b*) shows chosen intra- and intermolecular contacts.

The complex crystallized in non-centrosymmetric space group ($P2_12_12_1$) providing possible NLO response after pulsed-light irradiation of the complex.[9] This rare crystal packing is due to intra- and intermolecular interactions, and the strongest ones are formed by the nitrite and hydroxyl groups. The Hirshfeld surfaces[17,18] showing intermolecular contacts are depicted in Figure S1. The OH$^-$ ligand forms a contact with the hydrogen atom of a 3-CN-Py ligand [the O(2)···H distance is 2.34 Å, and the O(2)···H–C(3) angle is 169.6°] and a weak intramolecular hydrogen bond with an oxygen atom of NO^{2-} [the O(5)···H distance is 2.38 Å, and the O(5)···H–O(2) angle is 108°]. The interactions affect the Ru–OH bond length [1.923(3) Å], which is longer than that in known [RuNO(L)$_2$(NO$_2$)$_2$OH] complexes.[13,15,16] The oxygen atoms of NO^{2-} groups form intermolecular interactions with 3-CN-Py hydrogens (O···H distances in a range of 2.274–2.645 Å, and O···H–C angles of 115.5–164.0°) and contacts with aromatic rings (O···C distances are 2.922–3.209 Å) (Figure S2).

Photoinduced isomerism in the complex was studied by IR spectroscopy. For the generation of a metastable state, 445 nm light was chosen because this wavelength produced a maximum achievable MS1 population in the related complex [RuNOPy$_2$(NO$_2$)$_2$OH].[13] According to DFT calculations, the absorption bands of the [RuNO(3-CN-Py)$_2$(NO$_2$)$_2$OH] complex at 450–400 nm corresponded to charge transfer from hydroxyl and nitro ligands to the antibonding orbital of the Ru–NO coordinate (Figure S3). Light irradiation (445 nm) of the complex at 80 K led to the formation of a new band at 1749 cm^{-1} in the spectrum (Figure 2). The appearance of this band was accompanied by a decrease of the ν(NO) band of GS at 1873 cm^{-1}. In view of a characteristic shift of the $\nu(\mathrm{NO})_{\mathrm{GS}}$ band by 124 cm^{-1} to lower wavenumbers, the band was assigned to ν(NO) stretching vibrations of the MS1 isomer.[19,20] Similar spectroscopic properties were observed in related [RuNOL$_2$(NO$_2$)$_2$OH] complexes, where L = Py, γ-Pic.[13,15] In the MS1 isomer, the nitrosyl ligand is coordinated through oxygen atom with Ru–ON bond lengths of 1.867(3) and 1.888(1) Å and Ru–O–N angles of 177.6(2) and 164(2)° for Py and γ-Pic ligands, respectively. Based on the structural resemblance of the complexes, we assumed similar structural changes in the [RuNO(3-CN-Py)$_2$(NO$_2$)$_2$OH] complex. The maximum population of MS1 in [RuNO(3-CN-Py)$_2$(NO$_2$)$_2$OH] was ~10%, as measured based on a decrease in the area under $\nu(\mathrm{NO})_{\mathrm{GS}}$ before and after light exposure. In the case of an MS1 population of <50%, the structural parameters of MS1 in the presence of GS cannot be determined unambiguously.[21] Though nitro–nitrito isomerization in the mixed NO–NO$_2$ rhodium complex was reported,[22] it was not observed in the current case.

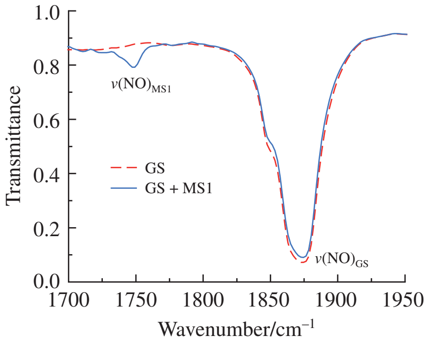

Figure 2 IR spectra of complex [RuNO(3-CN-Py)$_2$(NO$_2$)$_2$OH] before and after exposure to 445 nm light at 80 K.

The reversibility of the MS1 → GS back isomerization was studied by a combined IR and DSC technique. The heating of the sample to 200–210 K resulted in a decrease of the $\nu(\mathrm{NO})_{\mathrm{MS1}}$ band and an increase of $\nu(\mathrm{NO})_{\mathrm{GS}}$ due to the thermal decay of MS1 to GS (Figure 3). The reaction rate constants (k) at 200, 205 and 210 K are $(1.49\pm0.18)\times10^{-3}$, $(2.3\pm0.1)\times10^{-3}$ and $(4.12\pm0.1)\times10^{-3}$ s^{-1}, respectively, and the activation energy E_a and frequency factor lg k_0 are 35.47 ± 3.50 kJ mol^{-1} and 6.43 ± 0.89, respectively. The decay temperature T_d, which was calculated[23] from the Arrhenius law at $k = 1\times10^{-3}$ s^{-1}, is a useful parameter for comparing the MS1 thermal stability of different compounds measured by different techniques; the calculated T_d for [RuNO(3-CN-Py)$_2$(NO$_2$)$_2$OH] is 197 K.

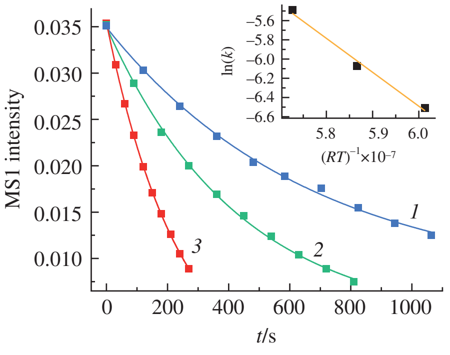

Figure 3 Decay of the ν(NO) band of MS1 at (*1*) 200, (*2*) 205 and (*3*) 210 K fitted by the one-exponential function. Insert: corresponding Arrhenius plot.

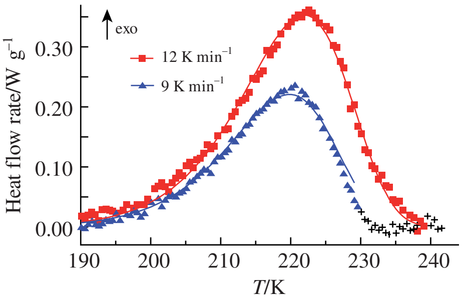

Figure 4 DSC curves of the reaction MS1 → GS measured at heating rates of 9 and 12 K min^{-1} and fitted by a first-order kinetic equation.

Since the kinetic parameters measured by IR spectroscopy were obtained in a narrow temperature range, the DSC curves were measured after the heating of MS1 (Figure 4). An exothermic effect at ~200 K corresponds to the exothermic reaction MS1 → GS. The DSC curves were fitted by the first-order kinetic equation $\mathrm{d}H/\mathrm{d}t = H_{\mathrm{tot}}\ (1-\alpha)\ k_0\ \exp[-E_{\mathrm{a}}\ (RT)^{-1}]$, where $\mathrm{d}H/\mathrm{d}t$ is the heat flow rate, H_{tot} is the total reaction enthalpy, and α is the conversion.[24] The calculated E_{a}, lg k_0 and T_{d} are 51.36 ± 1.03 kJ mol^{-1}, 10.49 ± 0.25 and 199 K, respectively. The kinetic parameters of the reaction MS1 → GS determined by DSC are more reliable; moreover, the values of E_{a} and lg k_0 are closer to those obtained for $[\mathrm{RuNOL_2(NO_2)_2OH}]$ compounds.[13,15]

An analysis of the complexes $[\mathrm{RuNOL}_x(\mathrm{NO_2})_{4-x}\mathrm{OH}]_{x-2}$ (L = N-donor heterocyclic ligands) showed that a variation of the type and quantity of the N-donor heterocyclic and nitrite ligands in the equatorial plane did not dramatically affect the thermal stability of MS1, which varied in a range of 185–212 K (Table S3). On the other hand, the electronegativity of the *trans*-to-NO ligand greatly affects the thermal stability of MS1.[9,25,26] There is no clear dependence of the MS1 population on the structure of a complex (Table S3), however, usually complexes with pyridine ligands show high MS1 population.[5,21] It was shown[2] that an increase of intermolecular contacts between the second coordination sphere of a complex and a nitrosyl ligand leads to a higher population of metastable states.

Thus, we synthesized a nitro–nitrosyl ruthenium complex with coordinated 3-cyanopyridine. This complex crystallized in non-centrosymmetric space group due to intermolecular interactions, which were analyzed using Hirshfeld surface maps. The dominant O···H/H···O, N···H/H···N and C···O/O···C contacts made a 60.3% contribution to the total Hirshfeld surface. The complex exhibits reversible light-induced nitrosyl linkage isomerism, with activation energy (E_{a}) and frequency factor (lg k_0) of Ru–ON → Ru–NO transformation of 51.36 ± 1.03 kJ mol^{-1} and 10.49 ± 0.25, respectively.

This work was supported by the Federal Agency for Scientific Organizations.

Online Supplementary Materials

Supplementary data associated with this article can be found in the online version at doi: 10.1016/j.mencom.2020.11.010.

References

1 P. Coppens, I. Novozhilova and A. Kovalevsky, *Chem. Rev.*, 2002, **102**, 861.
2 B. Cormary, S. Ladeira, K. Jacob, P. G. Lacroix, T. Woike, D. Schaniel and I. Malfant, *Inorg. Chem.*, 2012, **51**, 7492.
3 D. Schaniel, N. Mockus, T. Woike, A. Klein, D. Sheptyakov, T. Todorova and B. Delley, *Phys. Chem. Chem. Phys.*, 2010, **12**, 6171.
4 A. Y. Kovalevsky, G. King, K. A. Bagley and P. Coppens, *Chem. – Eur. J.*, 2005, **11**, 7254.
5 A. A. Mikhailov, E. Wenger, G. A. Kostin and D. Schaniel, *Chem. – Eur. J.*, 2019, **25**, 7569.
6 L. A. Kushch, E. B. Yagubskii, A. I. Dmitriev, R. B. Morgunov, V. A. Emelyanov, A. R. Mustafina, A. T. Gubaidullin, V. A. Burilov, S. E. Solovieva, D. Schaniel and T. Woike, *Phys. B: Condens. Matter*, 2010, **405**, 30.
7 D. Schaniel, M. Imlau, M. Weisemoeller, T. Woike, K. Kraemer and H.-U. Guedel, *Adv. Mater.*, 2007, **19**, 723.
8 J. Akl, C. Billot, P. G. Lacroix, I. Sasaki, S. Mallet-Ladeira, I. Malfant, R. Arcos-Ramos, M. Romero and N. Farfán, *New J. Chem.*, 2013, **37**, 3518.
9 A. Mikhailov, V. Vuković, C. Kijatkin, E. Wenger, M. Imlau, T. Woike, G. Kostin and D. Schaniel, *Acta Crystallogr., Sect. B: Struct. Sci., Cryst. Eng. Mater.*, 2019, **75**, 1152.
10 I. Asselberghs, K. Clays, A. Persoons, M. D. Ward and J. McCleverty, *J. Mater. Chem.*, 2004, **14**, 2831.
11 W. H. Hao, P. Yan, G. Li and Z. Y. Wang, *Dyes Pigm.*, 2014, **111**, 145.
12 G. A. Kostin, A. A. Mikhailov, N. V. Kuratieva, S. V. Tkachev, D. Schaniel and T. Woike, *Eur. J. Inorg. Chem.*, 2016, 4045.
13 G. A. Kostin, A. O. Borodin, A. A. Mikhailov, N. V. Kuratieva, B. A. Kolesov, D. P. Pishchur, T. Woike and D. Schaniel, *Eur. J. Inorg. Chem.*, 2015, **29**, 4905.
14 D. A. Freedman, D. E. Janzen and K. R. Mann, *Inorg. Chem.*, 2001, **40**, 6009.
15 G. A. Kostin, A. A. Mikhailov, N. V. Kuratieva, D. P. Pischur, D. O. Zharkov and I. R. Grin, *New J. Chem.*, 2017, **41**, 7758.
16 G. A. Kostin, V. Vorobyev, A. A. Mikhailov and N. V. Kuratieva, *J. Mol. Struct.*, 2019, **1193**, 334.
17 F. L. Hirshfeld, *Theor. Chim. Acta*, 1977, **44**, 129.
18 M. A. Spackman and D. Jayatilaka, *CrystEngComm*, 2009, **11**, 19.
19 D. Schaniel, T. Woike, L. Kushch and E. Yagubskii, *Chem. Phys.*, 2007, **340**, 211.
20 D. Schaniel, B. Cormary, I. Malfant, L. Valade, T. Woike, B. Delley, K. W. Krämer and H. U. Güdel, *Phys. Chem. Chem. Phys.*, 2007, **9**, 3717.
21 B. Cormary, I. Malfant, M. Buron-Le Cointe, L. Toupet, B. Delley, D. Schaniel, N. Mockus, T. Woike, K. Fejfarová, V. Petříček and M. Dušek, *Acta Crystallogr., Sect. B: Struct. Sci.*, 2009, **65**, 612.
22 D. Schaniel, E.-E. Bendeif, T. Woike, H.-C. Böttcher and S. Pillet, *CrystEngComm*, 2018, **20**, 7100.
23 Y. Morioka, A. Ishikawa, H. Tomizawa and E. Miki, *J. Chem. Soc., Dalton Trans.*, 2000, **54**, 781.
24 H. Zöllner, T. H. Woike, W. Krasser and S. Haussühl, *Z. Kristallogr. – New Cryst. Struct.*, 1989, **188**, 139.
25 R. D. Yamaletdinov and I. L. Zilberberg, *Eur. J. Inorg. Chem.*, 2017, **23**, 2951.
26 G. A. Kostin, A. A. Mikhailov, N. V Kuratieva, D. P. Pishchur and A. N. Makhinya, *New J. Chem.*, 2018, **42**, 18928.
27 O. V. Dolomanov, L. J. Bourhis, R. J. Gildea, J. A. K. Howard and H. Puschmann, *J. Appl. Crystallogr.*, 2009, **42**, 339.
28 G. M. Sheldrick, *Acta Crystallogr., Sect. A: Found. Adv.*, 2015, **71**, 3.
29 G. M. Sheldrick, *Acta Crystallogr., Sect. C: Struct. Chem.*, 2015, **71**, 3.

Received: 12th February 2020; Com. 20/6133